This article has been accepted for publication in a future issue of this journal, but has not been fully edited. Content may change prior to final publication. Citation information: DOI 10.1109/JPHOT.2016.2581980, IEEE Photonics Journal

Bound soliton fiber laser mode-locking without saturable absorption effect

Cheng-Jhih Luo, Sheng-Min Wang, and Yinchieh Lai

Dept. of Photonic & Inst. of Electro-Optical Engineering, National Chiao Tung-University, Hsinchu 300, Taiwan, R.O.C.

Abstract: Stable bound soliton laser mode-locking is experimentally demonstrated in an environmentally stable hybrid mode-locked Er-doped fiber laser without incorporating (equivalent) nonlinear saturable absorption effects. The laser is with a sigma-type cavity and exhibits a higher threshold for single to bound soliton mode-locking state transition. A nonlinear eigenstate analysis based on the master equation model and the concept of steady state lasing gain is developed to more physically explain the observed mode-locking state transition phenomena.

Index Terms: Fiber lasers, Mode-locked lasers, Ultrafast Lasers.

1. Introduction

Thanks to the advances of fiber laser technologies, mode-locked fiber lasers have become important platforms for investigating interesting nonlinear pulse propagation dynamics including the formation of bound solitons. In the literature, many of the reported experimental results on bound solitons are demonstrated on passive mode-locked fiber lasers [1-8] while only fewer of them are based on hybrid active/passive mode-locked fiber lasers [9-11]. The active harmonic mode-locking techniques offer the possibility to generate bound solitons at very high repetition rates. Generation of stable 10 GHz bound soliton pairs was first achieved in a hybrid FM mode-locked Er-doped fiber laser [9] and multiple bound soliton states have also been demonstrated by using a similar approach [10]. In most of these studies, the employed mode-locked fiber lasers are implemented with the passive polarization additive pulse mode-locking (P-APM) or the nonlinear polarization rotation mode-locking (NPRM) mechanism, which can produce an equivalent fast saturable absorption effect through the fiber nonlinearity [12]. Some of the later studies utilized real semiconductor, graphene, or carbon nanotube (CNT) saturable absorbers instead. Recent examples include a CNT mode-locked multi-wavelength ultrafast fiber laser [13] and a CNT mode-locked distributed ultrafast fiber laser with flexible fundamental repetition rate tuning capability [14]. Bound soliton states have also been observed in a fiber laser passively mode-locked by CNT [5]. The saturable absorption effect plays an important role for bound soliton formation in these lasers. The peak power of the pulse can be clamped at a certain level when the pulse energy is large enough due to the saturation of the nonlinear saturable absorption action. Further increasing of the pulse energy will lead to the instability of the single pulse state in the presence of the soliton effects and thus the optical pulse will tend to split for better stability [15]. After splitting, the multiple pulses can exhibit quite complicated interaction behavior due to the combined effects of all the linear and nonlinear pulse propagation terms in the laser cavity [1-11]. If the interaction is not strong enough to hold them together, they may get separated evenly such that the pulse repetition rate multiplication (or the harmonic mode-locking) will occur, where hysteresis phenomena may be observed during the transition [16]. In hybrid mode-locked fiber lasers, the bound soliton formation is achieved through the balance between the attractive force caused by phase modulation and the repulsive force caused by soliton interaction [10-11]. Interestingly, it has not been experimentally verified whether the bound soliton mode-locking state can still be found if there is no saturable absorption effect in the laser cavity. In the literature, hybrid mode-locked fiber soliton lasers with only Kerr nonlinearity and without equivalent fast saturable absorption have been reported [17-20]. The balance of the anomalous dispersion and Kerr nonlinearity enables the pulse to operate in the soliton regime and can lead to shorter pulse-width when compared to pure active mode-locked fiber

This article has been accepted for publication in a future issue of this journal, but has not been fully edited. Content may change prior to final publication. Citation information: DOI 10.1109/JPHOT.2016.2581980, IEEE Photonics Journal

lasers [19-22]. However, so far there has been no experimental report of bound soliton generation in these soliton fiber lasers. Recently we experimentally demonstrated bound soliton mode-locking in a hybrid FM mode-locked fiber laser without the saturable absorption effect [11]. The laser is environmentally stable through the use of a sigma-type laser cavity configuration [23,24], which is composed of a polarization maintaining (PM) reflection loop and a non-PM linear section with a Farady rotating mirror. The sigma-type cavity is with good environmental stability due to the use of the Farady rotating mirror for compensating the residual birefringence of the non-PM linear section. However, such a cavity design also makes the NPRM mechanism absent in the laser cavity. In some previous studies [25,26], extra Farady rotators have to be introduced in the non-PM linear section to implement the NPRM mechanism for passively mode-locking. In our study we use the original sigma-type cavity configuration to avoid the NPRM mechanism totally, so that we can more surely study the bound soliton mode-locking possibility without the saturable absorption effects. Detailed experimental results about the characteristics of the observed bound soliton mode-locking as well as the more interesting single to bound soliton state transition behavior will be presented in the present work. Numerical simulation as well as a nonlinear eigenstate analysis based on the master equation model will also be carried out to confirm the possibility of stable bound soliton formation. The obtained results agree nicely with the experimental observation and also more physically explain the observed single to bound soliton state transition phenomena.

2. Experimental Demonstration

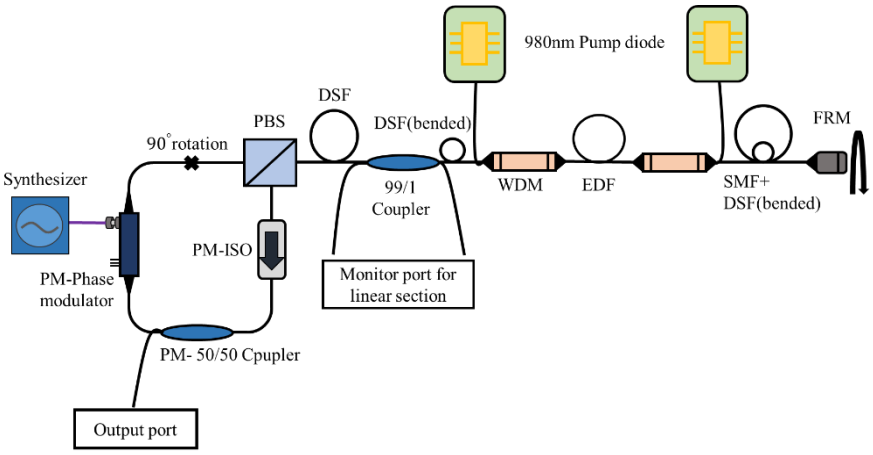

Fig. 1. Experimental setup of the sigma-type mode-locked fiber laser. FRM: Farady rotating mirror; SMF: Single mode fiber; DSF: Dispersion shifted fiber; WDM: Wavelength division multiplexing; EDF: Erbium-doped fiber; PBS: Polarization beam splitter; PM-ISO: Polarization maintain isolator.

The experimental setup of our hybrid FM mode-locked Er-doped fiber laser is shown in Fig. 1, in which a sigma-type cavity configuration is used. The mode-locked fiber laser can achieve environmentally stable operation through the combinational use of a polarization maintain (PM) fiber loop section and a non-PM linear fiber section. A Faraday rotator mirror is required for compensating the birefringence fluctuations experienced by the light waves propagating in the non-PM linear section [23,24]. The 2 m high concentration erbium-doped fiber (Leikki Er80 4/125) is pumped by two 980 nm laser diodes in both directions to act as the gain medium. A $LiNbO_3$ phase modulator (EOSPACE) is driven around 10 GHz for active mode-locking. The PM isolator is to ensure unidirectional propagation and the 50/50 PM coupler acts as the output port. The 99/1 coupler is used to monitor the optical output in the linear section and the 27 m dispersion shifted fiber (DSF) is incorporated to enhance the cavity Kerr-nonlinearity so that shorter pulses can be produced with better stability. The lasing wavelength is tuned to be near 1565nm by bending the

This article has been accepted for publication in a future issue of this journal, but has not been fully edited. Content may change prior to final publication. Citation information: DOI 10.1109/JPHOT.2016.2581980, IEEE Photonics Journal

DSF for inducing some wavelength dependent losses. The roundtrip cavity length is about 80m, corresponding to a cavity fundamental repetition rate of 2.5 MHz, and the net cavity dispersion is anomalous. The laser begins from CW lasing with the output average power around 0.2 mW. Single soliton mode-locking is achieved when the pump power of each diode is around 200 mW. The typical pulse width is about 2.8 ps and the output average power is 26 mW. Even shorter pulse-width can be expected if the cavity dispersion and other laser parameters are more optimized [9,18 -19]. The corresponding optical spectrum and auto-correlation trace are shown in Fig. 2. The 3 dB spectral bandwidth is about 1 nm and the time bandwidth product is 0.34, very close to the transform limit. The inset of Fig. 2(a) shows the pulse train traced by the oscilloscope with the span of 1 ns. The 100 ps pulse time period is confirmed and no pulse drop out is observed. Fig. 2(c) shows the measured RF spectrum with 50 dB super mode suppression ratio (SMSR) at the resolution bandwidth of 470 kHz, indicating the single soliton state is with very good stability under this power level.

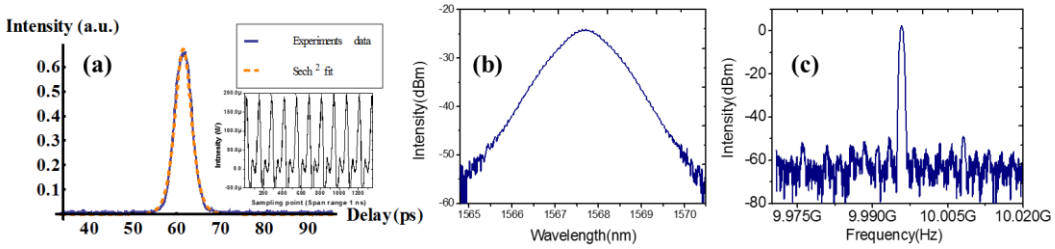

Fig. 2. (a) Auto-correlation trace and oscilloscope trace, (b) optical spectrum, and (c) RF spectrum centered at 9.9958 GHz with 50 MHz span and 470 kHz resolution bandwidth. The laser output power is 26 mW.

When the pump power of each diode is around 300 mW, the output power is increased above 36 mW. The auto-correlation traces begin to exhibit oscillating/splitting behavior, indicating that the single soliton state begins to become unstable. The optical spectra also begin to exhibit small oscillating behavior and the RF spectra begin to exhibit multiple side peaks around the 10 GHz main harmonic component. The spacing of the side peaks is about 90-100 kHz, which may be attributed to the relaxation oscillation effects. This indicates that the laser is now with larger fluctuations in the transition region. At this moment, if we slightly adjust the modulation frequency by a few kHz, the bound soliton mode-locking state can be observed. So both the unstable single and bound soliton mode-locking states can be observed in this transition region and we can switch between these states back and forth by simply tuning the modulation frequency. Eventually when the pump power of each diode is further increased to be around 540 mW, only the bound soliton state can be observed. Fig. 3(a) is the auto-correlation trace measured at the output average power of 66 mW. The three peaks in the auto-correlation trace indicate that there are two solitons bound together. Fig. 3(b) shows the optical spectrum with sinusoidal modulation. The dip in the center indicates that the phase difference between the two solitons is simply π [1,9]. This suggests that the physical mechanism for forming the bound soliton pair should be due to the balance of the repulsive force caused by soliton interaction and the attractive force caused by phase modulation and dispersion [9]. Fig. 3(c) shows the RF spectrum with the span of 1MHz, in which no clear side peak is observed, which indicates that the bound soliton state is with very good stability. Fig. 3(d) shows the RF spectrum with the full span of 26.5GHz at the output power of 74 mW. The pump power of each diode is now 570 mW, which is the maximum power level used in the present experiment. One can clearly see that the bound soliton state is operated at the 10 GHz repetition rate with excellent SMSR.

This article has been accepted for publication in a future issue of this journal, but has not been fully edited. Content may change prior to final publication. Citation information: DOI 10.1109/JPHOT.2016.2581980, IEEE Photonics Journal

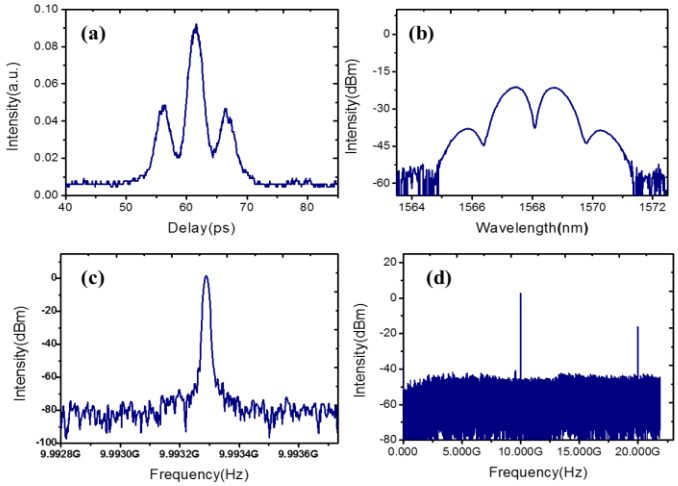

Fig. 3. (a) Auto-correlation trace, (b) optical spectrum, and (c) RF spectrum with 1 MHz span, measured at the output power of 66 mW. (d) RF spectrum with 26.5 GHz span measured at the output power of 74 mW.

Fig. 4(a) shows the bound soliton timing separation, the pulse width and their ratio as a function of the output power. Both of the pulse width and timing separation get slightly decrease when the power is increased while the ratio between them remains near constant. These are expected since when increasing the intracavity power, the increased nonlinearity will more shorten the pulse width. Physically the operation range of the soliton repelling force should be scaled with the pulse width. Therefore the steady state pulse separation is also reduced when the pulse width is reduced. Fig. 4(b) shows the bound pulse timing separation, the pulse width and the ratio between them as a function of the modulator driving power. Both the timing separation and the pulse width are found to be slightly decreased when the modulator driving power is increased [9]. This is again expected since when increasing the modulation depth, the pulse shortening force will also be increased. Table 1 shows the comparison of bound soliton state characteristics among different hybrid mode-locked fiber lasers. It can be seen that the studied laser exhibits a higher threshold for bound soliton formation in comparison to the hybrid NPRM mode-locked fiber lasers.

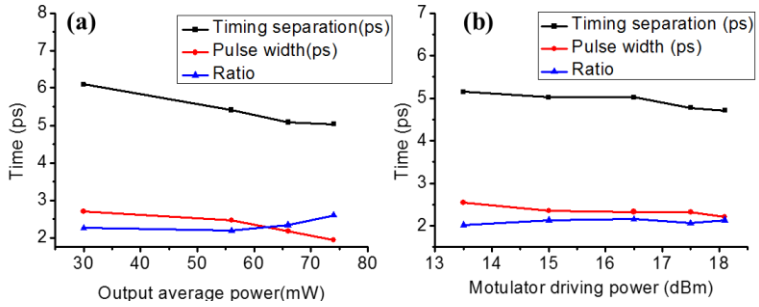

Fig. 4. (a) Bound pulses timing separation and pulse width versus laser output power under a fixed modulator driving power of 17 dBm. (b) Bound pulses timing separation, pulse width, and their ratio versus modulator driving power under a fixed output power of 69 mW.

This article has been accepted for publication in a future issue of this journal, but has not been fully edited. Content may change prior to final publication. Citation information: DOI 10.1109/JPHOT.2016.2581980, IEEE Photonics Journal

Table 1.
Comparison of bound state characteristics among hybrid mode-locked fiber lasers.

	Hybrid mode-locking		
Passive mode-locking method:	Soliton shaping	NPRM	NPRM
Repetition rate:	10 GHz	10 GHz	1 GHz
Pulse width: (ps)	2	1.3	9.6
Timing separation: (ps)	5.2	4	29
Output average power:	Up to 70 mW	Few mW	Few mW
Reference :	The present work	[9]	[10]

Experimentally we have observed up to 3 bound solitons in the studied laser. This suggests that the number of bound solitons can be increased by further raising the pump power [10]. Such bound soliton bursts may be suitable for photonic mm wave generation applications [27], in which the pulse separation tuning capability of the studied laser may also be useful. No bound soliton operation is observed at the fundamental frequency of 2.5 MHz since the studied laser needs strong enough active mode-locking effect for stable operation. Moreover, no Q-switched mode-locking behavior is observed in the studied laser when the cavity modulation frequency is detuned [28]. The use of phase modulation here may be one of the main reasons in contrast to the amplitude modulation case in [28].

3. Theoretical Results

To theoretically prove the possibility of bound soliton formation, we have performed the following numerical studies. For the sigma-type cavity structure, the optical pulses propagate bi-directionally in the non-PM linear section and uni-directionally in the PM ring section. Under the assumption of small round-trip changes, such a hybrid mode-locked fiber laser can be described by the master equation model given below: [29-31]

$$\frac{\partial u(T,t)}{\partial T} = \left(\frac{g_0}{1+\frac{\int |u|^2 dt}{E_s}} - l_0 \right) u + (d_r + j d_i)\frac{\partial^2 u}{\partial t^2} + j k_i |u|^2 u + jM\cos(w_m t)u \qquad (1)$$

Here $u(T,t)$ is the complex field envelop of the pulse, g_0 is the linear gain, E_s is the gain saturation energy, l_0 is the linear loss, d_r represents the effect of filtering, d_i is the group velocity dispersion coefficient, k_i is the self-phase modulation coefficient, M is the phase modulation depth, w_m is the angular modulation frequency, T is the large time scale denoted by the number of cavity roundtrip, and t is the short time scale. It should be noted only the Kerr nonlinear term is included and there is no nonlinear saturable absorption term in Eq. (1). This is because there is no equivalent saturable absorption action in the studied laser due to the sigma-type cavity configuration [24,25].

The simulation parameters for the studied laser are estimated by the following procedure. The unit of time t is assumed to be 0.5 ps. The amplifier linear gain and cavity linear loss coefficients are estimated from the experimental conditions. The dispersion coefficient is determined from the estimated roundtrip dispersion (-0.46 ps^2) with the roundtrip cavity length of 80 m. The modulation strength is estimated from the experimental driving power for the EO modulator and the modulation frequency is 10 GHz. The units for the peak power and saturation energy E_s are chosen according to the peak power and energy levels of the intra-cavity pulses so that the solutions can have a normalized peak power around 1. The self-phase modulation coefficient k_i and the filtering coefficient d_r are reasonably selected to match the experimental pulse width and other parameters. After normalization, the numerical values for all these parameters are given below: g_0

This article has been accepted for publication in a future issue of this journal, but has not been fully edited. Content may change prior to final publication. Citation information: DOI 10.1109/JPHOT.2016.2581980, IEEE Photonics Journal

= 2.6 to 10.1, l_0= 1.38, d_i= 0.9, M= 1.24, w_m= 0.0314, E_s= 2.6, k_i= 0.18 and d_r= 0.178. These parameters should be quite close to the actual experimental conditions of the studied laser.

Eq. (1) can be solved numerically based on the finite difference Crank-Nicolson method by propagating a suitable chosen initial pulse along the T direction. In our simulation, the initial condition is chosen to be one single or two bound hyperbolic secant pulses with the pulse-width = 0.88 ps, time-separation = 10 ps and normalized peak power = 0.01 and 0.09 for the single and bound soliton cases respectively. Fig. 5(a) shows the evolutionary plot for the single soliton mode-locking state by assuming an initial single secant pulse. The steady-state pulse width from simulation is about 2.8 ps, agreed with the experimental result reasonably. Fig. 5(b) shows the evolutionary plot when the intra-cavity power is about 3 times larger than the case in (a). One can see that now no stable single soliton solution is reached. In contrast, Fig. 5(c) shows the evolutionary plot with an initial bound secant pulse pair. The solution is stable with the steady-state bound pulse separation around 5.2 ps and the pulse width around 1.9 ps. These evolutionary simulation results provide direct numerical evidences that the single soliton mode-locking state will eventually become unstable when the intra-cavity power is increased and the bound soliton mode-locking state will become the stable operation state instead.

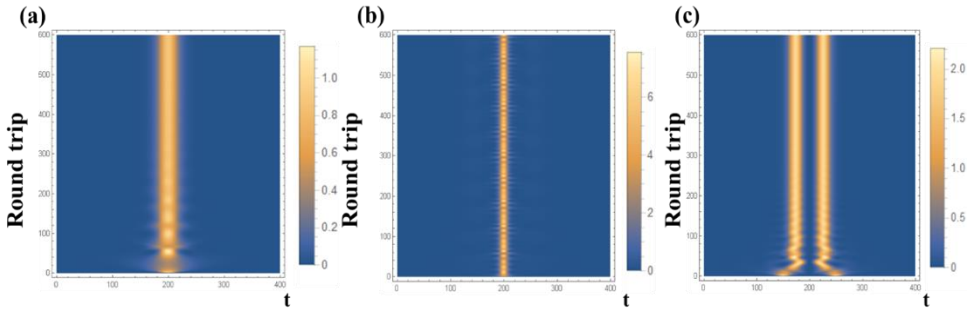

Fig. 5. Simulation results for (a) single soliton solution (g_0 = 4.37), (b) unstable single soliton state when the intracavity power is increased about 3 times (g_0 = 10.1), (c) stable bound soliton state under the same condition in (b). The steady state bound soliton pulse width and separation is 1.9 ps and 5.2 ps respectively.

To gain more physical insights about the observed stability/instability of the two mode-locking states, we have further developed a nonlinear eigenstate analysis to study the problem. The steady state solution of Eq. (1) can be reformulated as the nonlinear eigenstate problem in Eq. (2) with the constrain in Eq. (3).

$$jM\cos(w_m t)u + (dr + jd_i)\frac{\partial u^2}{\partial t^2} + jk_i\left|u^2\right|u = \lambda u \tag{2}$$

$$\frac{g_0}{1+\dfrac{\int\left|u^2\right|dt}{E_s}} - l_0 + \mathrm{Re}[\lambda] = 0 \tag{3}$$

The constrain in Eq. (3) comes from the balance of the net gain and loss at the steady state. Eq. (2) and (3) can be solved together numerically by using the root-finding algorithm like the Newton's method. The physical meaning of $\mathrm{Re}[\lambda]$ is the effective gain/loss coefficient produced by the combined effects of phase modulation, optical filtering, dispersion, and Kerr nonlinearity. Or equivalently, $-\mathrm{Re}[\lambda] = g_0/(1+\int|u|^2dt/E_s) - l_0$ is the required steady state lasing gain (relative to the constant loss) for the considered eigenstate. When - $\mathrm{Re}[\lambda]$ is smaller, the required steady-state lasing gain for the mode-locking state will be smaller. If there are many eigenstate solutions in the system, then the eigenstate with the smallest - $\mathrm{Re}[\lambda]$ will be the most stable steady state solution. This is because when this most stable state is lasing, the steady state lasing gain will be pinned at the lowest value when compared to other eigenstates. Thus other eigenstates will not be able to experience a high enough steady state lasing gain to maintain their steady state operation and will decay out eventually. Of course the above statements are only true when the required steady state lasing gain differences among these eigenstates are large enough. Otherwise the

This article has been accepted for publication in a future issue of this journal, but has not been fully edited. Content may change prior to final publication. Citation information: DOI 10.1109/JPHOT.2016.2581980, IEEE Photonics Journal

transient noises in the laser cavity can still excite the closely adjacent eigenstates which significantly enough to destroy the original eigenstate. Fig. 6 shows the calculated - $\mathrm{Re}[\lambda]$ for the two mode-locking states as a function of g_0, which is basically related to the steady state intracavity pulse energy according to $\int|u|^2dt \approx (g_0/l_0 - 1)E_s$, since $|\mathrm{Re}[\lambda]|$ is typically much less than l_0. For the considered numerical example, the range of g_0 from 2.6 to 10.1 will correspond to the output average power from 10 mW to the 73 mW with a linear relation. Clearly, when g_0 is increased, the - $\mathrm{Re}[\lambda]$ curves for both states gradually increase with different slopes. A cross-over occurs when a threshold value is reached. Below the threshold, the single soliton state is more stable, while above the threshold, the bound soliton state is more stable. Around the cross-over point the laser is expected to be not very stable due to the existence of closely adjacent eigenstates. Experimentally we do not observe obvious pulse energy jump or hysteresis phenomena during the transition in contrast to the pulse repetition rate multiplication case [16]. This agrees with the smooth transition behavior predicted in Fig. 6. One can see that the developed nonlinear eigenstate analysis here can provide more physical insights about the observed single to bound soliton state transition. The concept of the required steady-state lasing gain is also very useful for examining the stability/instability of the mode-locked lasing states in general [31].

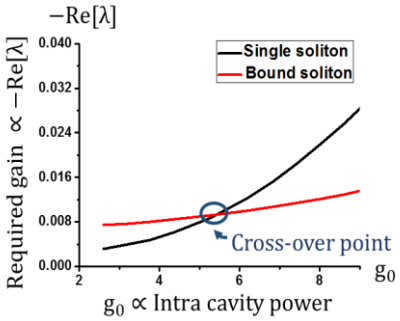

Fig. 6. Steady state lasing gain versus g_0 for the single and bound soliton states.

4. Conclusions

In conclusion, we have successfully generated stable bound soliton pairs in an environmentally stable hybrid mode-locked Er-doped fiber laser with a sigma-type fiber laser cavity. The fiber laser is without (equivalent) passive saturable absorption effects due to its optical design. Our results demonstrate for the first time that stable bound soliton mode-locking can still be achieved in a mode-locked fiber laser without saturable absorption. In comparison to other hybrid mode-locked fiber lasers with the passive nonlinear polarization rotation effect [9-10], the current laser exhibits a higher pulse energy threshold for transition from single soliton state to bound soliton state. This should be because the peak power of the intracavity pulses is now not limited by the nonlinear polarization rotation mechanism. One should be able to take advantages of these unique characteristics to build single as well as bound soliton mode-locked fiber lasers that can output larger pulse energies. We have also carried out a nonlinear eigenstate analysis based on the master equation model to confirm the observed single to bound soliton mode-locking transition possibility. The obtained results agree nicely with the experimental observation. The developed nonlinear eigenstate analysis here should also be very useful for studying other types of mode-locked fiber lasers.

Acknowledgements

This work was supported in part by the Ministry of Science and Technology of the Republic of China, Taiwan under Contract MOST-2221-E-009-152-MY3.

References

[1] D. Y. Tang, B. Zhao, D. Y. Shen, C. Lu, W. S. Man and H. Y. Tam, “Bound-soliton fiber laser,” *Phys. Rev. A,* vol. 66, pp. 033806, Sept. 2002.

[2] Ph. Grelu, F. Belhache, F. Gutty and J.-M. Soto-Crespo, "Phase-locked soliton pairs in a stretched-pulse fiber laser," *Opt. Lett.,* vol. 27, pp. 966-968, Jun. 2002.
[3] D. Y. Tang, B. Zhao, L. M. Zhao and H. Y. Tam, "Soliton interaction in a fiber ring laser," *Phys. Rev. E*, vol. 72, pp. 016616, Jul. 2005.
[4] B. Ortaç, A. Zaviyalov, C. K. Nielsen, O. Egorov, R. Iliew, J. Limpert, F. Lederer and A. Tünnermann, "Observation of soliton molecules with independently evolving phase in a mode-locked fiber laser," *Opt. Lett.,* vol. 35, pp. 1578-1580, May 2010.
[5] X. Wu, D. Y. Tang, X. N. Luan, and Q. Zhang, "Bound states of solitons in a fiber laser mode locked with carbon nanotube saturable absorber," *Opt. Commun.,* vol. 284, pp. 3615–3618, Jul. 2011.
[6] X. Liu, "Soliton formation and evolution in passively-mode-locked lasers with ultralong anomalous-dispersion fibers," *Phys. Rev. A,* vol. 84, pp. 023835, Aug. 2011.
[7] L. Yun and X. Liu, "Generation and propagation of bound-state pulses in a passively mode-locked figure-eight laser," *IEEE Photon. J.,* vol. 4, pp. 512-519, Apr. 2012.
[8] Z. Wang, L. Zhan, A. Majeed and Z. Zou, "Harmonic mode locking of bound solitons," *Opt. Lett.,* vol. 40, pp. 1065-16068, Mar. 2015.
[9] W.-W. Hsiang, C.-Y. Lin and Y. Lai, "Stable new bound soliton pairs in a 10 GHz hybrid frequency modulation mode-locked Er-fiber laser," *Opt. Lett.,* vol. 31, pp. 1627-1629, Jun. 2006.
[10] N. D. Nguyen and L.N. Binh, "Generation of high order multi-bound solitons and propagation in optical fibers," *Opt. Commun.,* vol. 282, pp. 2394-2406, Jun. 2009.
[11] C. J. Luo, S. M. Wang and Y. Lai, "10 GHz bound soliton mode-locking in an environmentally stable FM mode-locked Er-doped fiber soliton laser," in *Conference on Lasers and Electro-Optics, OSA Technical Digest (online)* (Optical Society of America, 2014), paper JTu4A.69.
[12] H. A. Haus, E. P. Ippen, and K. Tamura, "Additive-pulse modelocking in fiber lasers," *IEEE J. Quantum Electron.*, vol. 30, pp. 200-208, Jan. 1994.
[13] X. Liu, D. Han, Z. Sun, C. Zeng, H. Lu, D. Mao, Y. Cui and F. Wang, "Versatile multi-wavelength ultrafast fiber laser mode-locked by carbon nanotubes," *Sci. Rep*., vol. 3, pp. 2718, Sept. 2013.
[14] X. Liu, Y. Cui, D. Han, X. Yao and Z. Sun, "Distributed ultrafast fibre laser," *Sci. Rep*., vol. 5, pp. 9101, Mar. 2015.
[15] F. X. Kärtner, J. A. der Au, and U. Keller, "Mode-locking with slow and fast saturable absorbers—what's the difference?" *IEEE J. Sel. Topics Quantum Electron.,* vol. 4, pp. 159-168, Mar./Apr. 1998.
[16] X. Liu, "Hysteresis phenomena and multipulse formation of a dissipative system in a passively mode-locked fiber laser," *Phys. Rev. A*, vol. 81, pp. 023811, Feb. 2010.
[17] H. A. Haus and A. Mecozzi, "Long-term storage of a bit stream of solitons," *Opt. Lett.,* vol. 17, pp. 1500-1502, Nov. 1992.
[18] D. J. Jones, H. A. Haus, and E. P. Ippen, "Subpicosecond solitons in an actively mode-locked fiber laser," *Opt. Lett.,* vol. 21, pp. 1818-1820, Nov. 1996.
[19] F. X. Kärtner, D. Kopf, and U. Keller, "Solitary-pulse stabilization and shortening in actively mode-locked lasers," *J. Opt. Soc. Am. B,* vol. 12, pp. 486-496 Mar. 1995.
[20] H. A. Haus, "Mode-Locking of Lasers," *IEEE J. Sel. Topics Quantum Electron.*, vol. 6, pp. 1173-1185, Nov. 2000.
[21] K. Xu, R. Wang, Y. Dai, F. Yin, J. Li, Y. Ji and J. Lin, "Supermode noise suppression in an actively mode-locked fiber laser with pulse intensity feed-forward and a dual-drive MZM," *Laser Phys. Lett.,* vol.10, pp. 055108, Apr. 2013.
[22] J. Lee and J. H. Lee, "Experimental investigation of the cavity modulation frequency detuning effect in an active harmonically mode-locked fiber laser," *J. Opt. Soc. Am. B,* vol. 30, pp. 1479-1485, Jun. 2013.
[23] S. Yamashita, K. Hotate and M. Ito, "Polarization properties of a reflective fiber amplifier employing a circulator and a Faraday rotator mirror," *J. Lightwave Technol.,* vol. 14, pp. 385-390, Mar. 1996.
[24] T. F. Carruthers and I. N. Duling III, "10-GHz, 1.3-ps erbium fiber laser employing soliton pulse shortening," *Opt. Lett.,* vol. 21, pp. 1927-1929, Dec. 1996.
[25] T. F. Carruthers, I. N. Duling III and M. L. Dennis, "Active-passive modelocking in a single-polarisation erbium fibre laser," *Electronics Letters,* vol. 30, pp. 1051-1053, Jun. 1994.
[26] D. J. Jones, L. E. Nelson, H. A. Haus, and E. P. Ippen, "Diode-pumped environmentally stable stretched-pulse fiber laser," *IEEE J. Sel. Topics Quantum Electron.,* vol. 3, pp. 1076-1079, Aug. 1997.
[27] J. D. McKinney, S. Dongsun, D. E. Leaird and A. M. Weiner, "Photonically assisted generation of arbitrary millimeter-wave and microwave electromagnetic waveforms via direct space-to-time optical pulse shaping," *J. Lightwave Technol.*, vol. 21, pp. 3020-3028, Dec. 2003.
[28] Y. M. Chang, J. Lee, Y. M. Jhon, and J. H. Lee, "Q-switched mode-locking of an erbium-doped fiber laser using cavity modulation frequency detuning," *Appl. Opt.,* vol. 51, pp. 5295-5301, Jul. 2012.
[29] M. Horowitz, C. R. Menyuk, T. F. Carruthers and I. N. Duling III, "Theoretical and experimental study of harmonically mode locked fiber lasers for optical communication systems," *J. Lightwave Technol.,* vol. 18, pp. 1565-1574, Nov. 2000.
[30] W.-W. Hsiang, H.-C. Chang and Y. Lai, "Laser dynamics of a 10 GHz 0.55 ps asynchronously harmonic modelocked Er-doped fiber soliton laser," *IEEE J. Quantum Electron.*, vol. 46, pp. 292-299, Mar. 2010.
[31] S.Y. Wu, W.W. Hsiang and Y. Lai, "Synchronous-asynchronous laser mode-locking transition," *Phys. Rev. A,* vol. 92, pp. 013848, Jul. 2015.